Characterization of an All-Optical Device Based on Organic Materials

Hans-Martin KELLER, Mark Andreas BADER, Gerd MAROWSKY
Laser-Laboratorium Göttingen e.V.
Hans-Adolf-Krebs-Weg 1,
D-37077 Göttingen - GERMANY

We present numerical and first experimental results for an all-optical switching device. The device consists of a periodically modulated nonlinear waveguide, where so-called gap solitons stabilize the switching process. The fabrication of Bragg gratings in different polymeric films, e.g. poly(phenylene vinylene), polydiacetylene or polystyrene by excimer laser photoablation was tested. In preparation of further experiments numerical calculations were performed to characterize the device under realistic conditions, including position dependent index modulations and absorption losses. In further time-dependent simulations the transition from the reflecting to the transparent state was investigated in detail. As a main result, the threshold intensity turns out to be of the order of $100 \, \mathrm{MW/cm}^2$ for a realistic device layout and well-known materials, even in the presence of absorption losses. Furthermore, with this information an optimized, nonuniform Bragg reflector was designed and numerically characterized, considering the typical optical properties of monocrystalline polydiacetylene.

Introduction

All-optical nonlinear devices are able to process fast optical signals in communication lines without electrical control. One promising design concept is the so-called gap soliton switch, which consists of a periodically modulated planar or linear waveguide,[1−4] also called a Bragg reflector or distributed feedback mirror (especially in semiconductor lasers[5,6]). The modulation causes a coupling between the forward and backward traveling waves near the Bragg frequency ω_0 that results in the formation of Bragg or gap solitons. These soliton-like stable structures of the electro-magnetic field can be useful for pulse compression[4] or bistable switching.[3]

The numerical calculations presented here should prepare the ground for an experimental realization of the bistable switching device based on a planar polymeric waveguide. Although there has been a lot of theoretical work on this topic over the last decades,[1,7−15] there are only few experimental realizations of this concept. In 1996 Eggleton et.al. demonstrated pulse compression in a modulated glass fiber.[4] They gave a comparison between their experimental results and numerical simulations and found an excellent agreement. The first work on the topic of bistable switching was done by Sankey et.al.[3] In their work they investigated a silicon on insulator waveguide, where the optical nonlinearity is governed by free carrier generation. Even if the principles of operation could be demonstrated in their work, there are still open questions concerning the

influence of the free carrier lifetime, which is of the order of the pulse length (some nanoseconds). Further experiments with materials showing faster nonlinear response in the picosecond time domain should help to clarify the situation.

On the other hand, faster devices are also needed for technical applications. For both tasks polymeric materials, e.g. poly(phenylene vinylene) (PPV) or polydiacetylene (PDA), with high off-resonance third order optical nonlinearities ($\chi^{(3)} = 10^{-11} - 10^{-10}$ esu) are particularly suited.

In the last two decades several theoretical publications dealt with the complex behavior of such a device under different conditions. The aim of our investigation is to extend the knowledge to more realistic situations, including the effects of absorption losses and nonuniform gratings.[14,16] A nonuniform grating can accidentally be caused by inaccuracies during manufacturing. Therefore, the design of the device must guarantee proper operation even in the presence of small deviations.

Our analysis gives further indications to the fact, that uniform gratings tend to self-pulsations,[2,9] which are even more likely in the case of a slightly increased modulation strength in the middle of the device. Therefore, they are not applicable for switching purposes. A more stable operation can be achieved by reducing the grating strength in the middle. If this minimum is carefully designed, it can also reduce the switching threshold significantly, comparable to other types of nonuniform gratings.[17,18]

This publication shows some experimental results concerning the fabrication of Bragg gratings in different polymeric materials by excimer laser photoablation.[19] The main emphasis, however, is put on the numerical simulations, that are needed to prepare further measurements. Especially for polydiacetylene an optimized device layout is calculated and the influence of absorption losses on the switching process, i.e. stability and the threshold intensities, is investigated.

Experimental Setup and Theoretical Background

A. The Gap Soliton Switch

Figure 1 shows the layout of the gap soliton switch based on a planar polymeric waveguide. Two grating couplers are fabricated into a thin polymeric layer of about 1 μm thickness to couple the light beam in and out. The grating couplers can alternatively be replaced by prism couplers. The essential part of the device is the Bragg reflector between the two couplers, which can be a surface corrugation grating produced by etching or photoablation[19] or alternatively a bulk index modulation induced by photobleaching.[20] In both cases a periodic modulation of the effective index of refraction is achieved:

$$n_{eff}(z) = \overline{n} + \delta n \ \cos\left(\frac{2\pi}{d}z\right). \tag{1}$$

If the Bragg condition

$$\lambda \approx \lambda_0 = 2\overline{n}d \tag{2}$$

is satisfied, all backscattered partial waves are in phase and the structure is highly reflective (distributed feedback mirror).

So far, only the linear case has been described. At high intensities, however, the Bragg grating can get transparent due to non-linear optical effects.
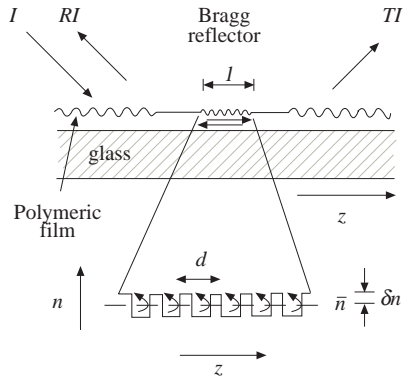
Figure 1. Layout of the gap-soliton switch.

B. Micro-Structuring of the Bragg Reflector

In introductory experimental work Bragg gratings were generated in poly(phenylene vinylene), polystyrene, and polydiacetylene by UV excimer laser photoablation. The experimental setup is shown in Figure 2. A grating mask with a period of 20 μm is illuminated by an excimer pulse of 20-30 ns and a wavelength of 193 or 248 nm. The mask is reduced by a factor of 50 onto the polymeric film producing a surface grating with a constant of $d = 380$ nm. As an example, a laser scanning microscope picture of a Bragg grating in PPV can be seen in Figure 3. In this case the energy density was about 2 J/cm^2 at the film surface. The light beam in the waveguide would travel perpendicular to the periodic structure at a wavelength of 1-1.5 μm, which is appropriate to satisfy the Bragg condition Eq. (2). Further details of the fabrication process can be found in an similar work done with the same setup.[19]
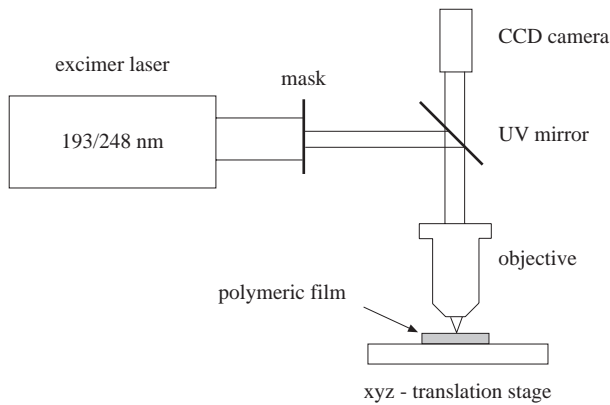
Figure 2. Experimental setup for photoablation.

The UV photoablation, that we use here, is a very general tool for structuring polymeric materials. The only requirement to be met by the material is showing some absorption in the deep UV, while all special chemical properties of the system are not considered. Another useful structuring method is photobleaching,[20] where the chemical structure of the system is changed during exposure. Since specific properties of the polymeric system are used, an appropriate wavelength has to be selected. On the other hand, the method has the advantage of less power consumption than photoablation where the material must be sputtered off by the light beam. However, in many cases both methods are applicable for micro-structuring of organic materials.

C. The Gap Soliton

In order to understand the operation of the bistable switch the concept of Bragg solitons must be introduced. A Bragg soliton is a stable structure of the electro-magnetic field,[2,21] similar to solitons in glass fibers.[22] In the special case of a zero group velocity (standing waves) they are called gap solitons, because their frequency must lie inside the so-called gap.
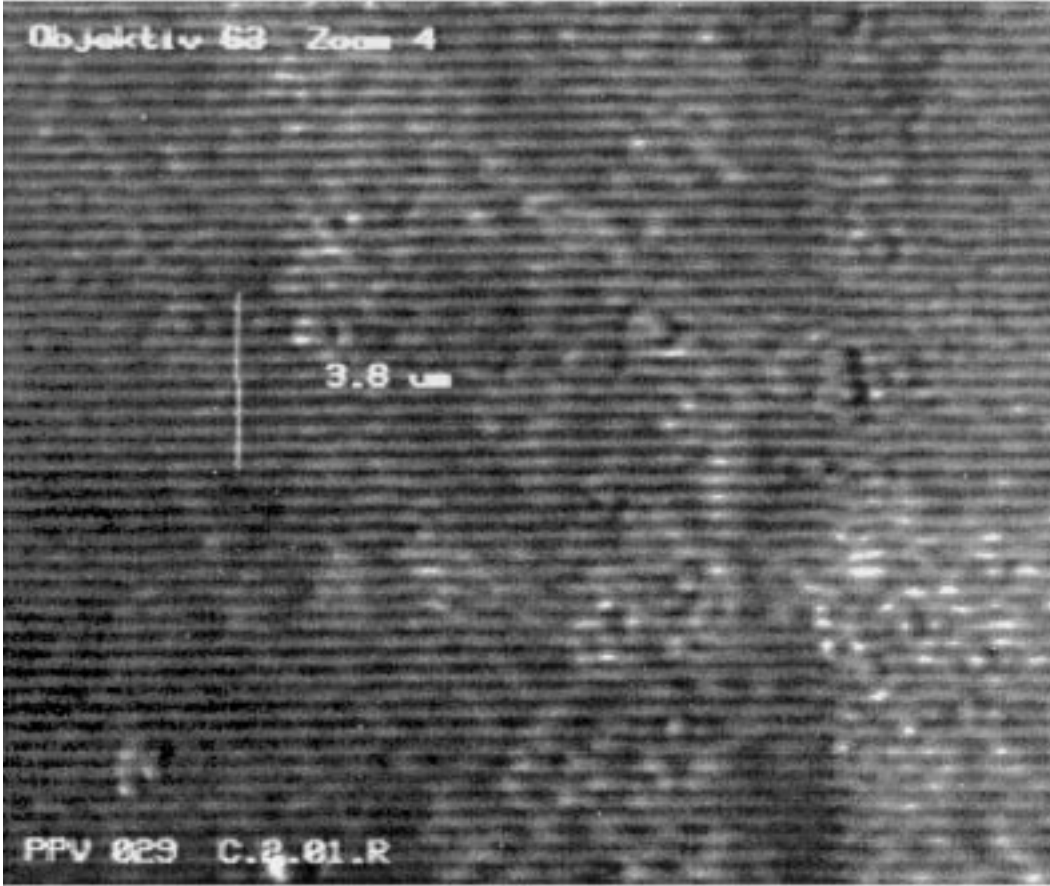
Figure 3. Laser-scanning microscope picture of a grating structure in PPV. The period is $d = 380$ nm.

The upper panel of Figure 4 shows the linear response of a Bragg reflector. At a wavelength close to $\lambda_0 = 2\overline{n}d$ the Bragg condition is satisfied and the structure is high-reflective, while it is transparent elsewhere. The reflecting region is called the gap referring to the band structure theory of semiconductor physics.[2] Its width $\Delta\lambda$ can be estimated from the modulation strength δn of the grating:

$$\frac{\Delta\lambda}{\lambda} \approx \frac{\delta n}{\overline{n}}. \tag{3}$$

At high intensities this gap is shifted to lower (higher) wavelengths for positive (negative) n_2 due to the nonlinear Kerr effect:

$$\overline{n}(I) = n_0 + n_2 I. \tag{4}$$

Therefore, at the wavelength marked with the dotted line the Bragg reflector becomes transparent for high field intensities, while it is reflecting in the linear case. This wavelength is appropriate for generating a gap soliton, such as the one shown in the lower drawing. In its center, at high intensities, the structure is

self-transparent and becomes high-reflective at both sides. So the gap soliton can be compared to a standing wave bounded by to mirrors, as indicated in the sketch.
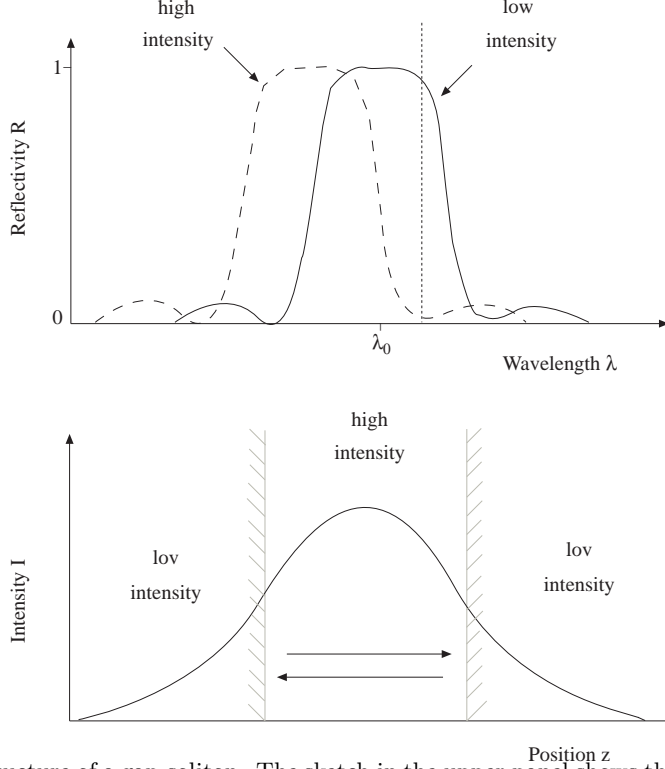
Figure 4. The field structure of a gap-soliton. The sketch in the upper panel shows the gap in the linear transmission spectrum, which is shifted to lower wavelengths at high intensities. The dotted line is the wavelength where a gap soliton can be created. The gap soliton can be considered (lower drawing) as a standing wave in a self-transparent region bounded by two distributed feedback mirrors.

The gap soliton switch has two stable internal states one without a gap soliton (reflecting, off state) and the other with a gap soliton inside (transparent, on state). The transition between these two states occurs spontaneously at two threshold intensities I_{on} and I_{off} (see below).

D. Coupled Mode Equations

For the numerical simulations we neglect the vector properties of the electromagnetic field and represent it as a complex scalar function:

$$E(z,t) = E_+(z,t)e^{-i(\omega_0 t - k_0 z)} + E_-(z,t)e^{-i(\omega_0 t + k_0 z)}. \tag{5}$$

Here $E_+(E_-)$ is the slowly varying envelope of the forward (backward) traveling wave, $k_0 = \pi/d$ the wave number, $\omega_0 = k_0 c/\overline{n}$ the frequency in the center of the gap, and c the velocity of light. With this assumption, the time dependence of the envelopes is governed by the following coupled equations:

$$
\begin{aligned}
+i\frac{\partial E_+}{\partial z} + i\frac{\overline{n}}{c}\frac{\partial E_+}{\partial t} + i\frac{\alpha}{2}E_+ + \kappa E_- + \Gamma_s|E_+|^2 E_+ + 2\Gamma_x|E_-|^2 E_+ &= 0 \\
-i\frac{\partial E_-}{\partial z} + i\frac{\overline{n}}{c}\frac{\partial E_-}{\partial t} + i\frac{\alpha}{2}E_- + \kappa E_+ + \Gamma_s|E_-|^2 E_- + 2\Gamma_x|E_+|^2 E_- &= 0,
\end{aligned}
\tag{6}
$$

5

Characterization of an All-Optical Device Based on Organic Materials, *H.M. KELLER, et.al.,*

where α is the absorption coefficient,

$$\kappa = \frac{\pi}{2d}\frac{\delta n}{n} \tag{7}$$

is the coupling constant, proportional to the index modulation δn, and

$$\Gamma_s = \Gamma_x = \frac{\pi}{2d\overline{n}^2}\chi^{(3)} \tag{8}$$

are the the self-phase and cross-plane modulation terms, proportional to the cubic nonlinear susceptibility $\chi^{(3)}$. Further details can be found in the review article of De Sterke and Sipe.[2]

Results and Discussion

A. The Non-Linear Characteristic

For time-independent calculations the coupled equations (6) are solved using a standard 8th order Runge-Kutta algorithm. The integration starts on the right-hand side at $z = z_1$ with a given outgoing amplitude $A_+(z_1)(A_-(z_1) = 0)$ and a constant detuning Ω, using

$$E_\pm(t,z) = A_\pm(z)e^{-i\Omega t}, \tag{9}$$

and is performed backwards down to $z = z_0$. Both $A_+(z_1)$ and Ω are varied to calculate the frequency and the intensity dependence.

Without optical nonlinearities ($\Gamma_s = \Gamma_x = 0$) the linear response can be calculated by varying the detuning only. A typical result is represented in Figure 5 for a Bragg reflector of length $\ell = 1$ mm, modulation strength $\delta n/\overline{n} = 1.06 \times 10^{-3}$, mean index $\overline{n} = 1.6$, and a center wavelength of $\lambda_0 = 1064$ nm. From Eq. (2) the grating constant can be calculated to be $d = 333$ nm, resulting in a total of 3000 grating periods.
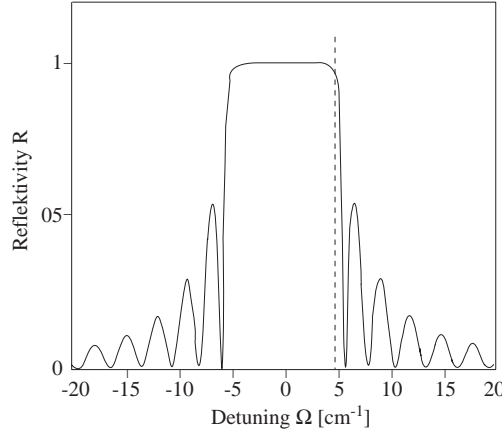
Figure 5. The linear reflectivity spectrum for the uniform grating (3000 periods, $\ell = 1$ mm, $\delta n/\overline{n} = 1.06 \times 10^{-3}, \overline{n} = 1.6, \lambda_0 = 1064$ nm). The vertical dotted line marks the detuning $\Omega = 4.8$ cm^{-1} used in subsequent calculations.

Including nonlinearities ($\Gamma_s = \Gamma_x \neq 0$) the reflectivity becomes intensity dependent, as can be seen from the nonlinear characteristic in Figure 6, where the detuning $\Omega = 4.8$ cm^{-1} is kept constant (dotted line in Figure 5). The assumed nonlinear susceptibility $\chi^{(3)} = 10^{-10}$ esu $= 1.40 \times 10^{-18}$ (V/m)$^{-2}$ is a typical off-resonance value for mono-crystalline PDA. For PPV the optical nonlinearity would be one order of magnitude lower, resulting in threshold intensities increased by one order.

6
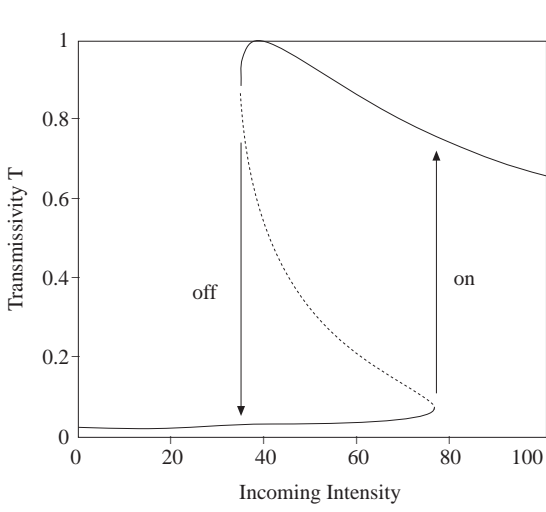
Figure 6. The nonlinear characteristic of the bistable switch for a constant detuning of $\Omega = 4.8$ cm^{-1}. There are two spontaneous transitions: from the reflecting to the transparent state (on) and vice versa (off).
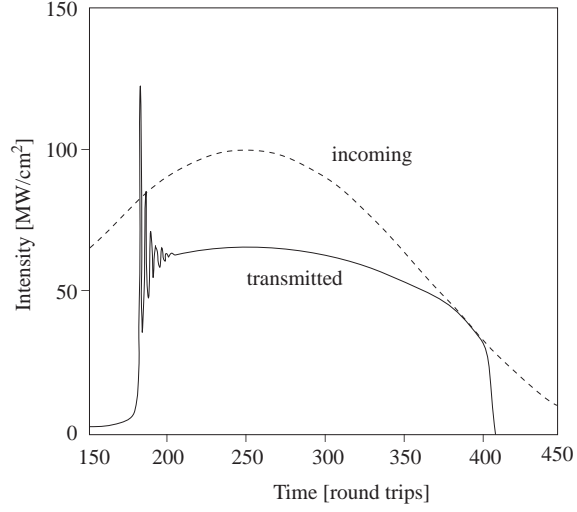
Figure 7. The time dependent switching behavior of the uniform grating. There are strong oscillations following the transition from the reflecting to the transparent state.

Interpreting the curve in Figure 6 most of the switching characteristics can be understood. The solutions indicated by a dotted line are unstable and will spontaneously transit to the upper or lower branch. So, if the incident power starts at low intensities and is increased up to $I_{on} = 77$ MW/cm^2, a spontaneous transition from the reflecting to the transparent state (on) occurs during which a gap soliton is created. The transition back to the reflecting state (off) occurs at a significantly lower intensity $I_{off} = 35$ MW/cm^2. For every incoming intensity between I_{on} and I_{off} there exist two stable states, one with a gap soliton (transparent) and the other without it (reflecting). This hysteresis behavior stabilizes the switching process and can be useful for noise rejection.

B. The Details of the Switching Process

To investigate the creation and destruction of the gap soliton in more detail time-dependent calculations were performed. A typical simulation with slowly varying input intensity is shown in Figure 7. If the incoming intensity reaches the upper threshold I_{on} the gap soliton is created and the device switches to the transparent state. The oscillations indicate, that the gap soliton needs some time to settle down. The settling time is about 10 round trip times ($t_r = 2\overline{n}\ell/c = 10.6$ ps), which adds up to a total of about 100 ps. Later in the simulation (right-hand part of the figure), when the incident power falls below the lower threshold I_{off} the gap soliton decays and the device adopts the reflecting state again.

Some remarks concerning the switching time may be helpful. The nonlinear response is assumed to be instantaneous, i.e. no relaxation times are included in the numerical calculation. To achieve a fast switching, the nonlinear response of the material should be faster than the round trip time of about 10 ps. Therefore, nonlinear processes relying on carrier generation or two-photon resonances ar not applicable, even if the optical nonlinearity is several orders of magnitude higher in those cases. In addition, close to a resonance the increased absorption is a strong drawback. Therefore, the nonlinear optical effect must rely on fast off-resonance electronic effects, otherwise the response of the device will be much slower.

As shown in the next section, the settling time of the gap-soliton can be reduced by an optimized

design of the Bragg reflector.

C. The Nonuniform Grating

There is no special reason to use a constant modulation strength $\delta n(z)$ in the Bragg reflector, instead, it has been shown earlier that a nonuniform grating shows interesting properties[14,16] and the threshold intensities can be reduced significantly.[17,18] In several numerical experiments we tried to optimize the switch for the optical parameters used above, by especially considering the upper threshold I_{on} under the secondary condition $I_{on}/I_{off} \approx 2$.

There are three simple topologies that can be used for the modulation strength $\delta n(z)$: (1) a maximum value in the middle, (2) a minimum value, or (3) the undefined case $\delta n = $ const. In the first case we did not see any stable switching in the time-dependent analysis. Obviously, the gap soliton is unable to settle down in the device, but a train of soliton-like pulses are radiated instead. This self-pulsation can also be seen in the undifned case (3) if the detuning approaches the middle of the gap.[2,9] Therefore both approaches are not suitable for a stable switching device.

The second case seems more promising. In Figure 8 a typical Bragg reflector with a minimum in the modulation strength is presented. Figure 8 (a) shows the band structure, i.e., the position dependent gap width $\frac{1}{\lambda}\frac{\delta n(z)}{\bar{n}}$. Inside the shaded region the device acts as a distributed mirror, while it is transparent outside. The minimum gap width is located in the center of the device. In Figure 8 (b) the linear response is plotted. Similar to the uniform grating there is a high-reflective gap, but at two well-defined wavelengths inside the gap ($\Omega_{res} = \pm 4.5$ cm^{-1}) the reflectivity goes down to zero. This is an indication for linear, Fabry-Perot like resonances.[16] At these frequencies there is a transparent region in the middle of the device (see left panel), bounded by two distributed mirrors. By controlling the device length and the minimum depth, the number, position and lifetime of the linear resonances can be controlled. These are the most important parameters, while the specific form of the modulation function s of less significance here, a step function could be used instead.
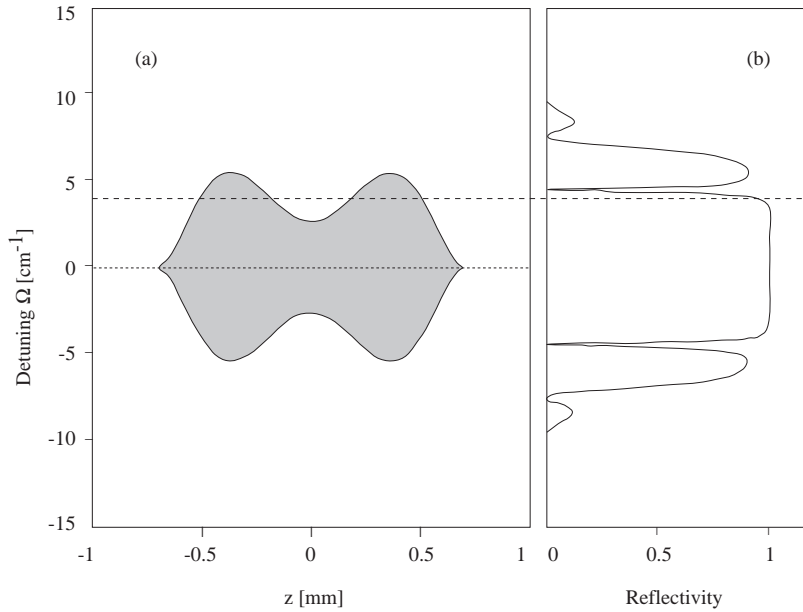
Figure 8. The band structure (a) and linear reflectivity (b) of the optimized nonuniform grating.

The nonlinear response of this optimized Bragg reflector is presented in Figure 9 for a detuning of Ω

= 4.0 cm^{-1} (dashed line in Figure 8) shortly below the linear resonance. Compared to the uniform grating the threshold intensities are reduced by a factor of 4, due to the influence of the linear resonance (I_{on} = 23 MW/cm^2, I_{off} = 9 MW/cm^2). In addition, the oscillations during the creating of the gap soliton are significantly reduced, but on the cost of a slightly slower response.
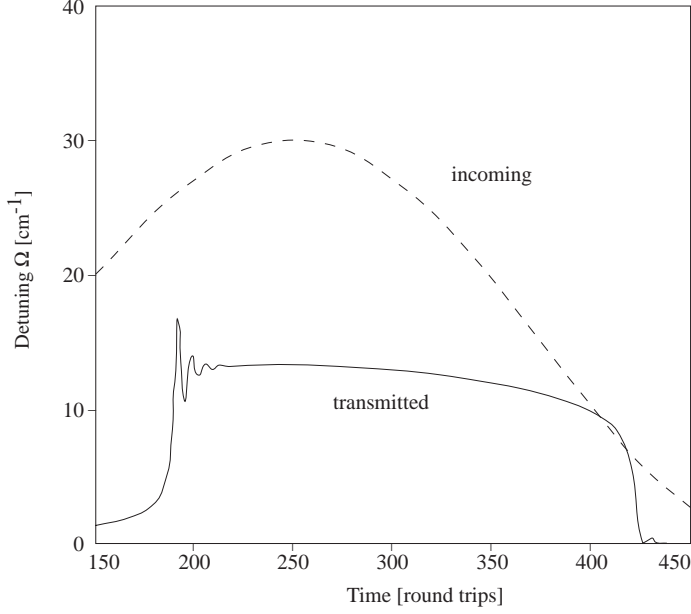
Figure 9. The time dependent switching behavior of the optimized grating. The oscillations and the threshold intensities are strongly reduced compared to the uniform grating (Figure 7).

This behavior can be understood by physical intuition. The longer the resonance lifetime (high-Q cavity) is, the higher are the internal fields compared to the incoming and outgoing intensities, but the longer it also takes to build up the internal mode. Therefore, the response time and the threshold intensities are both strongly correlated to the resonance lifetime. In the optimized grating presented here the resonance enhancement is carefully designed to reduce the threshold intensities significantly without slowing down the device too much.

D. The Influence of Absorption Losses

In thin planner waveguides scattering and absorption losses are a well known problem and therefore have to be considered in a realistic simulation. Typical values are of the order of some decibel per centimeter (dB/cm). Figure 10 shows the dependence of the threshold intensities I_{on} and I_{off} on the absorption coefficient α. For the uniform grating (right panel) a stable switching can be observed up to an absorption coefficient of about α = 0.4 mm^{-1} (17 dB/cm). At this value 50 % of the light power is lost during each round trip, but the switch still keeps working. This remarkable result shows, that the gap soliton switch is very unsensitive to absorption losses.
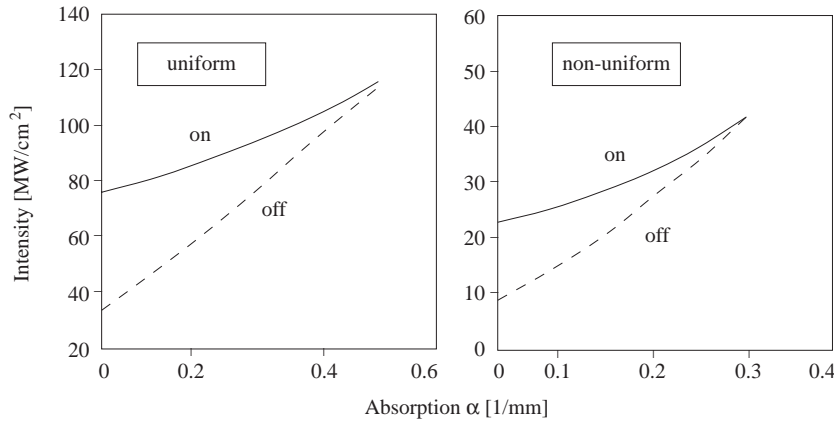
Figure 10. The influence of the absorption on the threshold intensities I_{on} and I_{off} for the uniform grating (left panel) and the optimized reflector (right panel).

The same is in principle true for the optimized, nonuniform grating, as can be seen in the right panel of Figure 10. In this case the tolerance for absorption losses is slightly lower, because the lifetime of the linear resonance is reduced by absorption, and thus the switching is inhibited. But even in this case the device is working for typical absorption losses of some decibel per centimeter.

Conclusion

In this work realistic numerical calculations were performed to investigate the nonlinear characteristics of the gap soliton switch for typical material constants of mono-crystalline PDA. The concept of a nonuniform grating, showing a minimum in the modulation function $\delta n(z)$, opens up the possibility to stabilize the switching through a linear Fabry-Perot like resonance with short lifetime. This helps to avoid self-pulsation and to reduce the threshold intensities significantly. By a careful design of the nonuniform grating, it is possible to control the lifetime and position of this resonance and thus to keep a balance between high thresholds and slow response. In addition it was proven, that typical absorption losses of some decibel per centimeter do not influence the operation of the device significantly. But still the polymeric films have to be of high quality, i.e. low surface roughnes and few impurities, to guide the light wave properly.

These theoretical predictions clearly show, that a fast bistable switch can be realized on the basis of well-known organic materials such as mono-crystalline polydiacetylene.

Acknowledgements:

References

1. W. Chen and D.L. Mills, Phys. Rev. Lett. **58**, 160-163 (1987).

2. C.M. de Sterke and J.E. Sipe, "Gap solitons" in *Progress in Optics XXXIII*, edited by E. Wolf, pp.203-260, North-Holland, Amsterdam, 1994.

3. N.D. Sankey, D.F. Prelewitz and T.G. Brown, Appl. Phys. Lett. **60**, 1427-29 (1992).

4. B.J. Eggleton, R.E. Slusher, C.M. de Sterke, P.A. Krug and J.E. Sipe, Phys. Rev. Lett. **76**, 1627-30 (1996).

5. H. Kogelnik and C.V. Shank, J. Appl. Phys. **43**, 2327-35 (1972).

6. R.G. Hunsperger, "Integrated Optics", Springer, Berlin Heidelberg, 1995.

7. M. Okuda and K. Onaka, Jap. J. Appl. Phys. **16**, 769-773 (1977).

8. H.G. Winful, G.D. Marburger and E. Garmire, Appl. Phys. Lett. **35**, 379-381 (1979).

9. H.G. Winful and G.D. Cooperman, Appl. Phys. Lett. **40**, 298-300 (1982).

10. H.G. Winful, Appl. Phys. Lett. **46**, 527-529 (1985).

11. A.B. Aceves and S. Wabnitz, Phys. Lett. A **141**, 37 (1989).

12. C.M. de Sterke and J.E. Sipe, Phys. Rev. A **42**, 2858-69 (1990).

13. C.M. de Sterke, Phys. Rev. A **45**, 2012-45 (1992).

14. J. He and M. Cada, Appl. Phys. Lett. **61**, 2150-52 (1992).

15. M. Picciau, G. Leo and G. Assanto, J. Opt. Soc. Am. B **13**, 661-670 (1996).

16. J.E. Sipe, L. Poladian and C.M. de Sterke, J. Opt. Soc. Am. A **11**, 1307-20 (1994).

17. C.M. de Sterke and J.E. Sipe, Opt. Lett. **18**, 269-271 (1993).

18. N.G.R. Broderick, C.M. de Sterke and J.E. Sipe, Opt. Comm. **113**, 118-124 (1994).

19. H. Schmidt, J. Ihlemann and B. Wolff-Rottke, "Excimer laser micromachining based on dielectric masks" in *Laser Materials Processing and Machining*, Proc. SPIE 2246, pp.67-73, 1994.

20. L. Palchetti, Q. Li, E. Giorgetti, D. Grando and S. Sottini, Appl. Opt. **36**, 1204-12 (1997).

21. D.N. Christodoulides and R.I. Joseph, Phys. Rev. Lett. **62**, 1746-49 (1989).

22. D. Marcuse, "Theory of Dielectric Optical Waveguides", Academic Press, San Diego, 2nd ed., 1991.